

MEASUREMENTS OF DECAY AND SNAPBACK IN Nb₃Sn ACCELERATOR MAGNETS AT FERMILAB*

G. Velev[†], G. Ambrosio, G. Chlachidze, J. DiMarco, S. Stoynev and T. Strauss, Fermilab, Batavia, Illinois

Abstract

In recent years, Fermilab has been executing an intensive R&D program on Nb₃Sn accelerator magnets. This program has included dipole and quadrupole models and demonstrators for various programs and projects, including the HL-LHC accelerator upgrade project. A systematic study of the field decay and snapback during the injection portion of a simulated accelerator cycle was executed at the Fermilab Magnet Test Facility. This paper summarizes the recent measurements of the MQXFS1 short quadrupole model and discusses the results of some previously measured Nb₃Sn magnets at CERN.

INTRODUCTION

In the late 1980's, after the first several years of operation of the Tevatron collider, dynamic effects in the main superconducting dipoles were observed. Since then the control of these effects has become an important part of the operation of any superconducting machine.

The most significant changes are observed in the allowed field components of the magnets, for example in the normal sextupole (dodecapole) component of the main dipoles (quadrupoles). These changes are especially important during the time of beam injection, when the strong variation of the sextupole field in the main dipoles can generate a significant growth in chromaticity. This change in the sextupole typically presents itself as slow decay from the hysteresis curve during injection dwell. In the next step, when the magnet current is ramped to accelerate the beam, a fast snapback of the sextupole component to the hysteresis curve is observed.

Since 2002, Fermilab has been executing an intensive measurement program studying decay and snapback in superconducting accelerator magnets. This program includes models and demonstrators in dipole and quadrupole configuration containing NbTi and Nb₃Sn superconductors for projects [1, 2] and programs [3, 4]. While the decay and snapback in the NbTi magnets are well documented and understood, the new results for Nb₃Sn magnets are somehow showing a deviation from this experience [5-7]. For example, recent CERN result on Nb₃Sn magnets, measured at 1.9 K, showed inverse decay during the injection dwell. These results were obtained on the 11 T 2-m dipole models (MBHSP and MBHDP) [8] and 1.2-m short quadrupole models (MQXFS) intended for the high luminosity IR upgrade [9].

At the Fermilab Magnet Test Facility, we performed new tests and reanalyzed some old data from the 11 T dipole

* Work supported by Fermi Research Alliance, LLC, under contract No. DE-AC02-07CH11359 with the U.S. Department of Energy.

[†] velev@fnal.gov

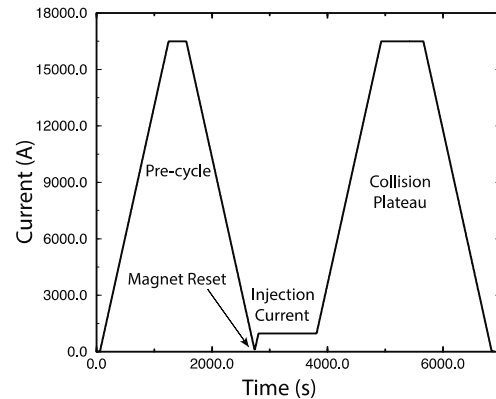


Figure 1: Typical current profile used in the measurements.

program. Unlike CERN, the results [10] show decay and snapback following the same trend as NbTi. After comparing measurement programs, one of the differences found between Fermilab's and CERN's measurements is the spatial length of the field harmonics integration. At Fermilab, we measured only the harmonics in the body of the magnet, while the CERN measurements were integrated over the entire 1.5 m length of the magnet, including the body and the ends.

This paper supplements the findings of previously published manuscripts on the topic of decay and snapback measurements. It presents new measurements of the decay and snapback in the MQXFS1 short quadrupole model [11]. For this magnet we performed a longitudinal scan specifically measuring the gradient and normal dodecapole (b_6) in the body and in the lead and return ends.

FIELD DEFINITION AND MEASUREMENT SYSTEM

A standard way to express the field in the magnet aperture is with the harmonic coefficients defined in a series expansion

$$B_y + B_x = B_2 \cdot 10^{-4} \cdot \sum_{k=1}^n (b_k + ia_k) \left(\frac{x+iy}{R_{ref}} \right)^{k-1} \quad (1)$$

In equation (1), B_x and B_y are the field components in Cartesian coordinates, b_n and a_n are the $2n$ -pole normal and skew coefficients at reference radius R_{ref} , normalized by the main field (B_i) and scaled by a factor of 10^4 in order to report the harmonics in convenient "units." The reference radius $R_{ref} = 50$ mm for these measurements was defined as 2/3 of the magnet aperture.

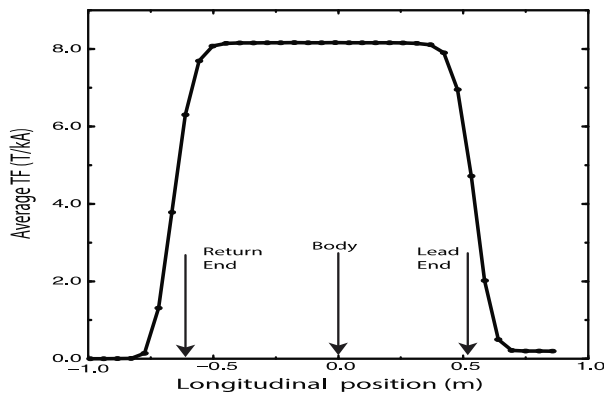


Figure 2: Magnet transfer function versus the longitudinal (z-)position in the magnet. The arrows show where the center of the 220-mm probe was positioned.

The magnet was excited following the current profile (Fig. 1) that emulates the operation of LHC. The maximum current of the precycle and collision plateau is set to 16,500 A. The linear ramp to plateau is set to 14 A/s. The injection dwell is at 960 A for 1000 s. One of the deviations from the LHC current profile is that the current ramp after the injection dwell does not at the beginning follow parabolic, and later, exponential acceleration to 14 A/s. This deviation might affect the snapback length, but not the amplitude.

To measure the field components, we used the standard rotating coil technique. The measurement probe is built on circuit board technology [12] and has two sensitive regions of integration: a long one with a length of 220 mm and a short one with a length of 110 mm. For these measurements, we used the 220 mm probe. The center and the ends of the magnet were determined based on the transfer function distribution (Fig. 2). For the lead and return ends, we positioned the center of the 220 mm probe at -0.65 m and +0.55 m, respectively. Three accelerator profiles were executed according to the profile shown in Fig. 1. These three measurements represent well the dynamic processes in the MQXFS1 short quadrupole model.

The integration component of the data acquisition system is based on ADC with a digital signal processor board and has the capacity to continuously gather data at high rotational probe speeds [13]. To reduce the noise generated by the mechanical vibrations of the rotational parts, we used a relatively low probe speed of 1 Hz.

All measurements were run at a temperature of 1.9 K LHe.

FIELD DECAY

During the injection dwell, the most significant changes can be observed in the normal dodecapole component and to a lesser extent in the main gradient field (B_2). Figure 3 shows B_2 during the injection dwell at the three measured positions. One can conclude that the magnet body and return end show no changes in the gradient field with time while for the lead end measurement, B_2 increases by 7.5

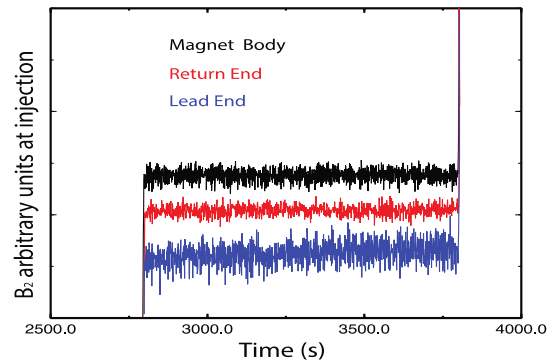


Figure 3: Magnet gradient (B_2) at injection versus time.

units (0.075%). We noted that the noise of this measurement is approximately 2.5 times larger than expected, which needs additional investigation.

To parameterize the decay in the dodecapole field (b_6) components, we used the double exponential form as proposed in [14].

$$\Delta b_6^{dec}(t) = b_{6,1} \cdot \left(1 - e^{-\frac{t}{\tau_1}}\right) + b_{6,2} \cdot \left(1 - e^{-\frac{t}{\tau_2}}\right). \quad (2)$$

In Eq. 2, two exponential forms are needed to fit with the fast and slow modes of the decay. The equation is similar to what is used to describe the decay dependence in LHC dipoles [14] and LHC Nb₃Sn models [8,9].

Figure 4 shows the result of the fits with Eq. 3 at the three measured positions. The magnet body and return end show a normal behavior of the decay with different ratios between the fast and slow modes. One can see that at the return end, b_6 increases much faster at the beginning of the injection dwell.

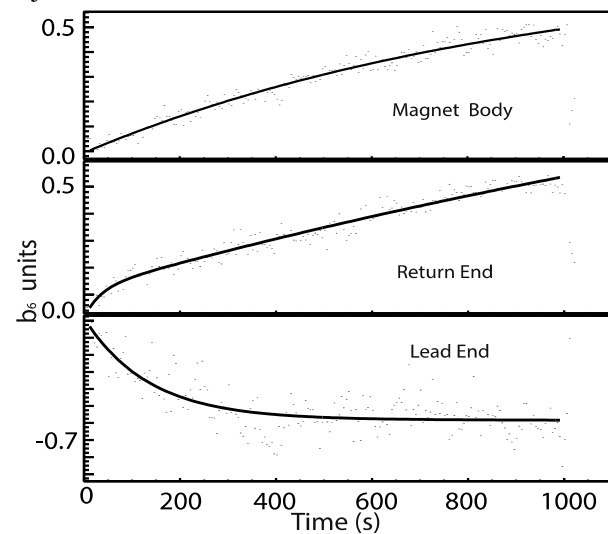


Figure 4: Dodecapole decay (b_6) at injection measured at the magnet body, return, and lead ends. The solid lines represent the result of the parametrization with Eq. 3.

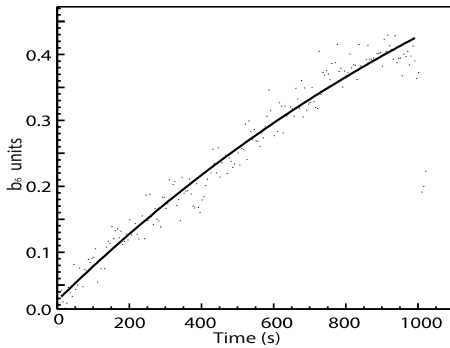


Figure 5: Dodecapole decay at injection averaged over the three measured positions.

The measurement at the lead end shows inverse behavior, similar to what was seen in the LHC Nb3Sn models. Again, we should stress that we observed a large noise in the lead end measurement, which may point to some particularities of the DAQ or mechanical systems and which needs to be better understood. If this is proven to be a real effect, we should look at the magnet splices and how they induce current imbalances among the strands in the magnet cable.

Having measurements at three different positions, we averaged the b_6 decay amplitudes, weighting them according to the gradient field. The result of this procedure gives a normal decay behavior as shown in Fig. 5, which is expected due to the large weighting given to the magnet body field in the averaging procedure.

DODECAPOLE DECAY

In our analysis, we describe the snapback time dependence by a half Gaussian distribution, where $t_{sb} = 0$ at the beginning of the current ramp:

$$\Delta b_6^{sb} = \Delta b_6(t_{inj}^{end}) \cdot e^{-\left(\frac{t}{t_1}\right)^2} \quad (3)$$

We found that Eq. 3 describes well the snapback in the case of the Tevatron dipoles [1]. It can be shown that Eq. 3 is mathematically equivalent to the LHC definition of the

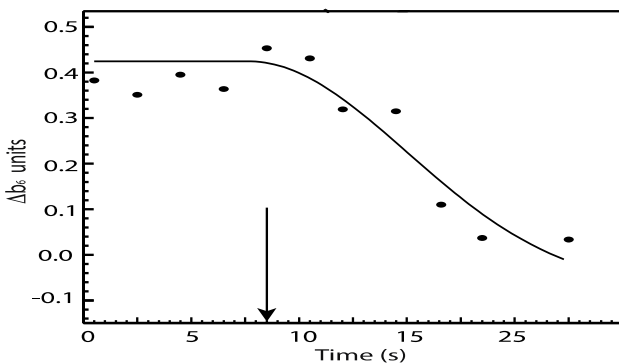


Figure 6: Observed snapback in the magnet body. The arrow is pointing at the beginning of the beam acceleration, which triggers the snapback.

development of snapback (see Ref. [14], Eq. 10) assuming a parabolic increase of the current with time at the start of beam acceleration.

Figure 6 shows the averaged snapback in the magnet. The snapback amplitude $\Delta b_6 = 0.42$ units and duration $t_1 = 8$ s are consistent with what we have reported for the NbTi quadrupoles [15].

CONCLUSION

In this paper, we presented a summary of the most recent measurements of the dynamic effects in the MQXFS1 short quadrupole model performed at Fermilab. We measured the gradient and dodecapole field components during the injection dwell at three positions in the magnet: the body and the lead and return ends. The decay in the body and return end shows normal behavior while the decay at the lead end shows inverse behavior, similar to what was seen in the LHC MQXFS3 and MQXFS04 models [9]. We should note that the lead end measurement needs additional investigation due to the increased noise in the probe signals. For the duration of the injection dwell, we averaged b_6 from the measurements and the result is consistent with the normal behavior of the decay and snapback that was observed in previous Fermilab measurements.

REFERENCES

- [1] G. Velev *et al.*, “Measurements of the Persistent Current Decay and Snapback Effect in Tevatron Dipole Magnets”, *IEEE Trans. Appl. Supercond.*, vol. 17, no. 2, 2007, pp. 1105-1108.
- [2] L. Bottura, L. Walckiers, R. Wolf, “Field Errors Decay and “Snap-Back” in LHC Model Dipoles”, *IEEE Trans. Appl. Supercond.* vol 7, no. 2, pp. 602-605, 1997.
- [3] A. V. Zlobin *et al.*, “Development of Nb3Sn 11 T Single Aperture Demonstrator Dipole for LHC Upgrades”, *Proc. 2011 PAC*, New York, pp. 1460-1462.
- [4] E. Todesco *et al.*, “Design studies for the low-beta quadrupoles for the LHC luminosity upgrade”, *IEEE Trans. Appl. Supercond.*, vol. 23, no. 3, Jun. 2013, Art. no. 4002405
- [5] M. Haverkamp, “Decay and Snapback in Superconducting Accelerator Magnets”, PhD Thesis, University of Twente, Netherlands, 2003.
- [6] G. Annala *et al.*, “Measurements of Geometric, Hysteretic and Dynamic Sextupole in Tevatron Dipoles”, Fermilab note TD-04-043. Available: <http://www-tdserver1.fnal.gov/project/TDlibrary/TD-Notes/2004%20tech%20Notes/TD-04-043.pdf>
- [7] L. Bottura *et al.*, “A Scaling Law for Predicting Snap-back in Superconducting Accelerator Magnets”, *Proc. of European Accelerator Conf.* Lucerne, Switzerland, 2004, pp. 1609-1611.
- [8] S. Izquierdo Bermude *et al.*, “Decay and Snapback in Nb3Sn Dipole Magnets”, *IEEE Trans. Appl. Supercond.*, vol. 27, no. 4, 2017, Art. no. 4002306.
- [9] S. Izquierdo Bermude *et al.*, “Magnetic Analysis of the MQXF Quadrupole for the High Luminosity LHC”, *IEEE Trans. Appl. Supercond.*, vol. 29, no. 5, 2019, Art. no. 4901705.

- [10] G. Velev *et al.*, “Measurements of Dynamic Effects in FNAL 11 T Nb₃Sn Dipole Models”, *IEEE Trans. Appl. Supercond.*, vol. 28, no. 3, 2018, Art. no. 4005904.
- [11] G. Chlachidze *et al.*, “Performance of the first short model 150 mm aper-ture Nb₃Sn quadrupole MQXFS for the high-luminosity LHC upgrade”, *IEEE Trans. Appl. Supercond.*, vol. 27, no. 4, Jun. 2017, Art. no. 4000205
- [12] J. DiMarco *et al.*, “Application of PCB and FDM Technologies to Magnetic Measurement Probe System Development”, *IEEE Trans. Appl. Supercond.*, Vol. 23, No. 3, 2013, Art. no. 9000505.
- [13] G. V. Velev *et al.*, “A fast continuous magnetic field measurement system based on digital signal processors”, *IEEE Trans. Appl. Supercond.* vol. 16, no. 2, pp. 1374–1377, June 2006.
- [14] N. J. Sammut *et al.*, “Mathematical formulation to predict the harmonics of the superconducting Large Hadron Collider magnets”, *Phys. Rev. ST Accel. Beams* 10, 082802, 2007.
- [15] G. Velev *et al.*, “Magnetic Field Measurements of LHC Inner Triplet Quadrupoles Fabricated at Fermilab”, *IEEE Trans. Appl. Supercond.* vol. 17, no. 2, pp. 1109–1112, July 2006.